

Protein-Based Disk Recording at Areal Densities beyond 10 Terabits/in.²

S. Khizroev, R. Ikkawi, N. Amos, R. Chomko, V. Renugopalakrishnan, R. Haddon, and D. Litvinov

Abstract

The concept of optical protein-based memory has been of interest since the early 1970s. Yet, no commercially available protein-based memory devices exist. This review presents an analysis of the main challenges associated with the practical implementation of such devices. In addition, the discussion includes details on the potential of using the unparalleled properties of photochromic proteins by creating an optical data storage disk drive with unmatched features and, particularly, record-high data densities and rates.

Introduction

It is a historical time for the information storage industry. Conventional technology is facing an inevitable end because of a fundamental limit to the laws of scaling. Because the superparamagnetic limit was recently reached, the industry was forced to abandon longitudinal magnetic recording in favor of perpendicular recording.¹⁻³ Perpendicular recording offers a factor of three to five improvement in the data density, which makes it an incremental solution to the growing demand for information storage. A number of technologies have been proposed to further defer the limit. The two most popular alternatives are patterned media⁴⁻⁶ and heat-assisted magnetic recording.⁷⁻¹⁰ These technologies promise to defer the superparamagnetic limit beyond 1 terabit (Tb)/in.². However, because of the large number of open questions associated with any of the proposed technologies, it might still be premature for a reliable forecast on how far and how fast any of these alternatives could take the industry.^{11,12} The industry does not have a consensus on the technology to pursue beyond three to five years from today. Nonetheless, the demand for higher data density of storage and mem-

ory devices is growing exponentially, especially with the ever-increasing use of the Internet, explosive growth of broadband communication, increasingly complex multimedia mobile devices, and rapid expansion of on-demand databases serving multinational businesses.¹³

The concept of optical protein-based memory has been of interest since the early 1970s.¹⁴ Yet, no commercially available protein-based memory devices exist. In this review, we analyze the main challenges associated with the practical implementation of such devices. In addition, we discuss the feasibility of exploiting the truly unparalleled properties of photochromic proteins by realizing an optical data storage disk drive with unmatched features and, particularly, record-high data densities and rates.

It appears that much of the early research on protein-based electronic devices was conducted in the former Soviet Union during the Cold War, in an effort to jump ahead of Western computing technologies, mostly for military purposes.¹⁵ Although most results remain classified, Soviet work on bacteriorhodopsin (BR) has become widely known and has triggered extensive

research in this field in Western countries and Japan.¹⁶⁻¹⁹

BR is a purple-colored protein found in microbes that live in harsh environments such as salt marshes and salt lakes. In such extreme conditions, few organisms other than these microbes, called *Halobacteria salinarium*, can survive. Their notoriously bright purple color explains the color of the natural and artificial saline basins and salt lakes as seen from an airplane (Figure 1). When nutrients become scarce, cell membranes that are rich in BR come into play. They serve as a light-converting enzyme that keeps the organism's lifecycle going. Specifically, as a photochromic protein, BR converts light energy into chemical energy through a proton-pumping action across the *Halobacterium salinarium* cell membrane.²⁰ In this way, BR acts as a protein powerhouse that turns on in times of famine, changing color from purple to yellow as it absorbs light.²¹

For billions of years, evolution has perfected the chemical and physical functions of BR, with the protein often performing better than synthetic materials ever could. BR can function under conditions of intense light, survive in salt marshes, and withstand temperatures as high as 140°C and pressures above 300 GPa. This unprecedented thermal and chemical stability is probably the main reason that BR has become the most attractive candidate for a protein-based building block of future electronic devices.²² Moreover, the BR molecule is extremely simple and efficient.

BR is found in the form of two-dimensional (2D) crystal patches integrated into the halobacterial cell membrane, as illustrated in Figure 2. Each patch is a self-assembled array of BR molecules. The tendency of molecules of BR to self-assemble



Figure 1. Photograph of salt lakes in Australia. The origin of the purple color is attributed to the abundant presence of bacteriorhodopsin. Image credit: Cheetham Salt Limited.

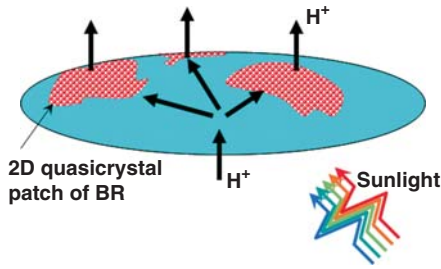


Figure 2. Schematic of a halobacterial cell covered with patches of self-assembled two-dimensional (2D) arrays of bacteriorhodopsin (BR) molecules. The light-driven proton-pumping process is illustrated.

into a crystal lattice explains the protein's unique stability.²³ Whereas the stability of the protein is determined by the collective assembly, the unique optical properties of BR are inherent to individual molecules. The characteristic diameter of each BR molecule is only 2 nm. Each molecule acts as a light-driven proton pump with an unprecedented (high) quantum efficiency of approximately 60%.²⁴ Such high quantum efficiency implies that less than two photons are necessary to trigger each proton-pumping process. The molecules are perfect optical cells/switches.

One ambitious goal has been to learn to implement this (almost-quantum) optical cell to leapfrog advances in electronics and, particularly, information-storage-related technologies. Furthermore, with the modern advances of genetic engineering, any additional features could be custom-tailored to suit practically any other specific technology requirement.^{25,26} Finally, the feasibility of cost-effective mass production through genetic engineering is also not implausible.

A three-dimensional (3D) structure of a BR molecule is shown in Figure 3. The image was created with the popular free-ware application RasMol.²⁷ The structure of the molecule was elucidated with an accuracy of 3.5 Å by the Henderson group.^{28,29} BR consists of 262 amino acids, from which a propeptide of 13 amino acids is cleaved. Even a simple picture such as this can display the main features of BR. Its structural signature, the amino acid chain folded into seven transmembrane helices, is represented as seven gray strands. Several key groups are highlighted: The light-absorbing retinal chromophore (linked to Lys-216 through a protonated Schiff base) is shown in red and is in its ground-state (all-trans) configuration. Also shown are the important residues Asp-85 (yellow), Arg-82 (purple),

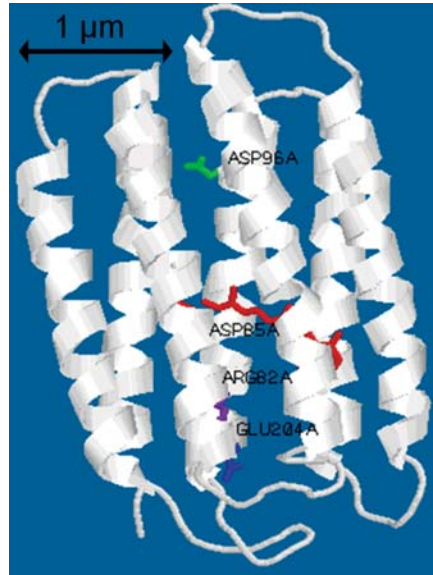


Figure 3. Three-dimensional structure of the BR molecule. The light-absorbing retinal chromophore (linked to Lys-216 through a protonated Schiff base) is shown in red and is in its ground-state (all-trans) configuration. Also shown are the important residues, Arg-82 (purple), Glu-204 (blue), and Asp-96 (green).

Glu-204 (blue), and Asp-96 (green). The structural changes during the photocycle result in the irreversible proton-transport or proton-pumping mechanism.³⁰ The structural changes in BR are preceded by deprotonation of the Schiff base.³¹ The longest side of the molecule is on the order of only 2 nm.

Photocycle of BR as the Key to Enable Information Storage beyond a 10 Tb/in.² Density

When BR absorbs a photon of light, it passes through a cycle of structural changes, that is, the photocycle of BR.^{32,33} The key result of the changes is the isomerization from all-trans to 13-cis of the retinal chromophore bound at Lys-216.³⁴ Each change in the molecular structure is referred to as an intermediate. Figure 4 shows the intermediates in the photocycle of BR at room temperature. The intermediates are identified with capital letters, and the numbers in parentheses indicate the wavelengths (in nanometers) of the absorption maxima. The thin black arrows indicate the transitions (between the respective intermediates) through thermal fluctuations, whereas the thick colored arrows reflect the photochemically induced transitions. The color of each thick arrow represents the color of the excitation frequency.

Naturally, these conformational light-induced changes are also temperature-dependent, implying that an intermediate can be stabilized ("frozen") at a certain temperature, usually below -10°C (specific to each intermediate). At temperatures below the freezing temperature, the transition to the next intermediate becomes suppressed. The characteristic relaxation times (lifetimes) of some of the intermediates at room temperature are shown next to the respective thin arrows. The photocycle with intermediates can be treated as a state diagram with intermediates presented as states. Each intermediate has its own absorption spectrum, and thus, intermediates (states) can be optically distinguished from each other. The characteristic absorption spectra of some of the key intermediates (in information-storage-related applications) of BR at room temperature are shown in Figure 5.

The following key properties of the photocycle of BR should be highlighted with regard to information-storage-related applications:

- The photocycle of BR consists of several branches.³⁵ The two most significant (for information-related applications) branches are the core and branched photocycles. During its normal function, the BR molecule remains in the core photocycle. The intermediates in the branched photocycle are not populated at physiological conditions.³⁶ As described in a following point, for the molecule to go into the branched photocycle, the protein should be exposed to a certain sequence of light.
- In general, the ground state of BR, or the bR state, consists of a 6:4 mixture of the D and B intermediates. Upon exposure to light, all of the protein molecules transition into the B intermediate. From there, they transition into the core photocycle, as illustrated in Figure 4.
- In the core photocycle, every transition between any two adjacent intermediates is reversible, with the exception of the transition from M2 to M1. The transition from M2 to M1 is responsible for the irreversible proton transport during the photocycle (deprotonation and reprotonation).³⁷ It should be noted that the M2 and M1 intermediates have practically indistinguishable absorption spectra. Consequently, the combination of M2 and M1 is often referred to as the M state.
- The core photocycle could be used for dynamic short-term (volatile) memory applications, such as random-access memory and devices for fast nondestructive optical processing.³⁸ In this case, the ground state (bR) and the complex M state are usually used as the two binary states, that is, "0" and "1," respectively. The life-

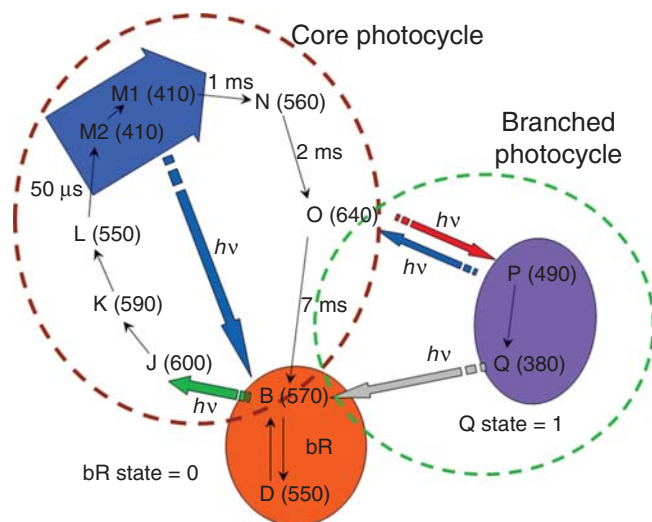


Figure 4. Schematic of the photocycle of BR at room temperature. bR is the ground state, and the intermediates (states) are identified with capital letters. The numbers in parentheses indicate the wavelengths (in nanometers) of the absorption maxima. The thin black arrows indicate the transitions (between the respective states) through thermal fluctuations, whereas the thick colored arrows reflect the photochemically induced transitions. The color of each arrow represents the color of the excitation frequency.

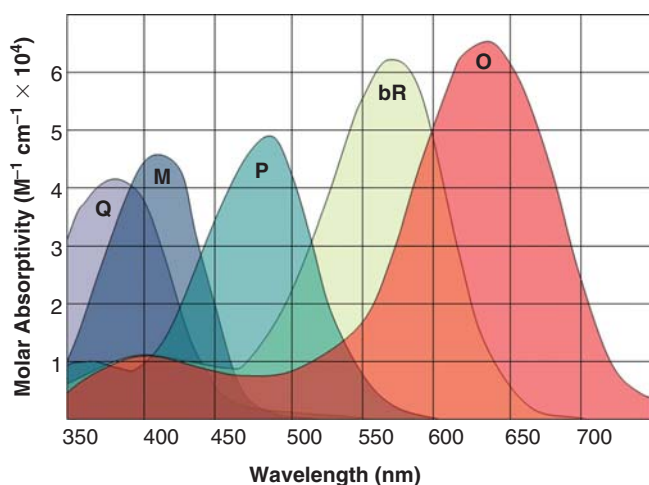


Figure 5. Schematic illustrating typical absorption spectra of the five key states, bR, M, O, P, and Q, in the photocycle of BR.

time of the M state at room temperature varies from approximately 1 s for the wild-type BR to a few minutes for certain variants of BR, such as D96N. The wild-type BR is the original form found in nature, whereas variants are genetically engineered mutants of BR. Today, both types, the wild-type BR and BR variants, are commercially available.³⁹ Furthermore, as mentioned in the Introduction, with the modern advances of genetic engineering, it is very likely that the lifetime of the M state could be further optimized to fit specific applications. However, because the

lifetime of the M state is still relatively short, the core photocycle cannot yet be used for nonvolatile memory applications.

■ It is the branched photocycle that is being considered for most long-term nonvolatile memory applications. Nature itself manufactured a device with a photocycle that is almost ideally suited for long-term information-storage applications.⁴⁰ In this case, the two binary states (i.e., 0 and 1) are represented by the ground state (bR) and either the P or Q intermediate in the branched cycle. The branched photocycle originates at the O intermediate, that

is, after deprotonation has taken place. When the protein is illuminated by red light, it branches off from O to P. Then, the protein thermally converts from P to Q. The Q intermediate is isolated from the core photocycle by a relatively large energy gap, which underlies the nonvolatile memory application of BR. To transition from the Q intermediate back to the bR state in the core photocycle, the protein is exposed to blue light. The process results in the reisomerization of the chromophore to the all-trans configuration and the return of the protein to the ground (bR) state. As illustrated in Figure 5, the bR state and the Q intermediate have quite different absorption spectra and, thus, can be optically distinguished.

■ To implement 3D volumetric optical memory, various paging principles have been proposed to access information in selected regions during both writing and reading steps. With paging, the intersection of two beams of light is used to select specific regions. This often makes 3D recording devices relatively bulky and complex. In contrast, without the need to use sophisticated paging methods to read information, the branched photocycle could also be used to enable relatively cost-effective 2D protein-based information storage with areal densities above 10 Tb/in.². This review article focuses on the 2D approach.

■ The characteristic time of the optically induced transitions between certain intermediates can be on the order of a few picoseconds. This implies that the fundamental limit of the data rate in a protein-based system is far beyond the fundamental limits for competing magnetic or semiconducting technologies.⁴¹⁻⁴³

Two-Dimensional Protein-Based Information Storage Systems

Three-dimensional protein-based memory technologies have been extensively studied for over a decade.^{20,44,45} However, no commercial products based on this approach have yet been developed. For protein-based memory to be able to compete with conventional technologies, it is necessary to demonstrate the feasibility of achieving substantially higher data densities and/or data rates. A two-dimensional implementation of protein-based recording might be a more adequate and convincing way to demonstrate and take advantage of the unmatched characteristics of the photochromic protein compared to conventional alternatives. In this implementation, a disk coated with a thin protein could be used similarly to a magnetic or optical recording disk. As shown in Figure 6, in this case, a recording trans-

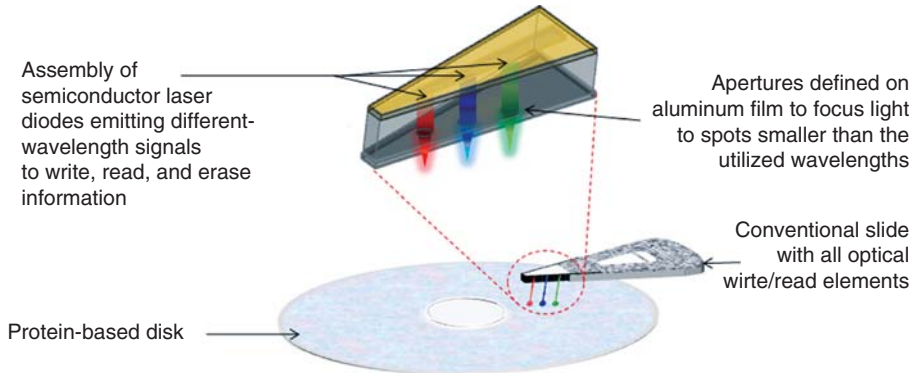


Figure 6. Schematic illustrating protein-based disk recording implementation.

ducer consisting of write and read elements scans the disk at a fixed separation between the disk and the transducer. The goal would be to demonstrate substantially higher areal data densities and perhaps data rates compared to magnetic and optical disk recording. In the following sections, we discuss the principles of writing and reading information in the case of protein disk recording.

Two-Step Write Mechanism

As mentioned earlier, to enable non-volatile information storage, it is necessary to use the branched photocycle, with the binary states 0 and 1 defined as the bR (ground) state (in the core photocycle) and either the P or Q intermediate (in the branched photocycle), respectively. There are many different ways to implement write and read mechanisms in protein disk recording.⁴⁶ We discuss some of the most obvious ways to accomplish these tasks. To set off the branched photocycle, two diodes with two different wavelengths, namely, green and red, need to be used. First, the green light is used to convert the protein from the ground state to the O intermediate. Then, the red light is used to convert BR from O to the P intermediate in the branched photocycle (within a few picoseconds), from which it thermally transitions into the stable Q intermediate. To put this process into practice and implement a write process in protein-based disk recording, the following two-step mechanism can be used:

As the first step (absorption of the first photon), a certain track can be selected through exposure to the green light. In this case, the green diode is on for the duration of one disk rotation (period). The characteristic time for the rotation period is in the range of a few milliseconds, depending on the rotation rate. For example, it would take approximately 4

ms for the rate of 15,000 rotations per minute (rpm). As a result of this exposure, the protein along the selected track is driven to the O intermediate, as shown in Figure 7a. During the second step (absorption of the second photon), the red diode is used to record certain information in the track. The red laser is turned on and off to record 1's and 0's, respectively, in the bit regions along the track, as shown in Figure 7b. The relaxation time of the O intermediate is on the order of 7 ms, which is longer than the period of the disk rotation (3 ms) and thus perfectly suited for the described recording two-step write mechanism. To further increase the efficiency of the recording process, faster rotation of the disk might be preferred. However, to maintain an adequate temporal separation between the two photon-absorption events, it might be necessary to spin the disk in the idle mode (with all three diodes off) for one or more rotations before the second-step photon is fired.

Finally, to erase information in a bit, the blue diode is turned on. When exposed to the blue light, the protein in the exposed bit region converts back to the ground (bR) state, as shown in Figure 7c.

Genetic engineering might become a cost-effective tool to further increase the recording efficiency. In this case, the goal of the genetic engineering would be to design a BR variant with a substantially increased yield of the O intermediate.⁴⁷ Because the O intermediate is the gateway to the branched photocycle, by increasing chances for the protein to transition into this intermediate, one also increases the efficiency of the described write process. The efficiency of the write process is defined as the fraction of photons in the source that result in a successful transition into the branched photocycle.

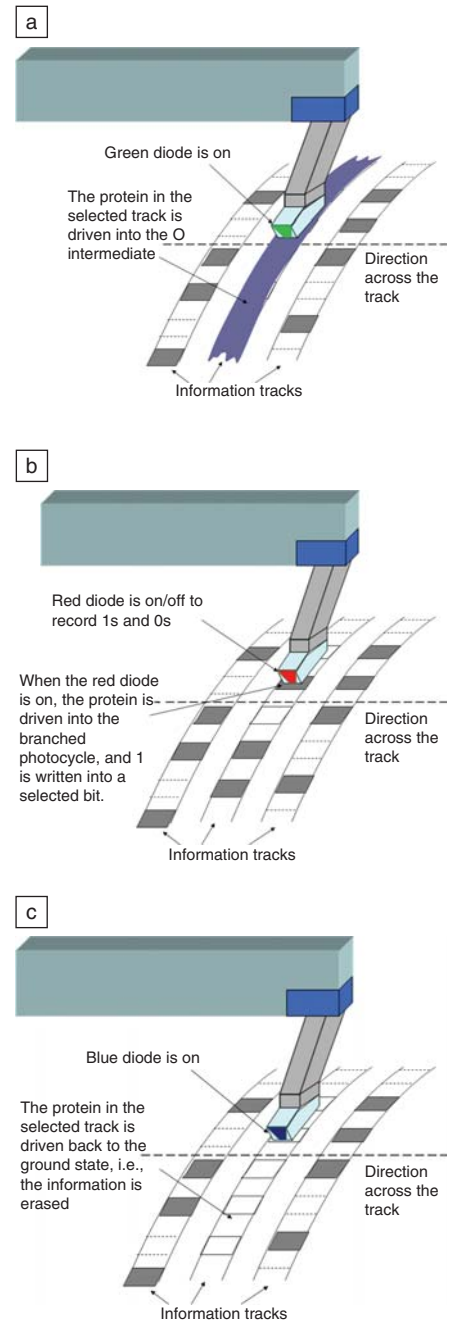


Figure 7. Schematics illustrating the two-step write process: (a) A selected track is exposed to green light to drive the protein in this region to the O intermediate. (b) The information is recorded by turning the red diode on and off. If a certain bit is exposed to red light, the protein in this region transitions into the branched photocycle, and the binary 1 is recorded. Otherwise, with the red diode off, the binary 0 remains written in the bit. (c) When the blue diode is on, the information in a bit is erased; that is, the protein in the bit converts back to the ground state (i.e., the binary 0 state).

It should be noted that, with this relatively trivial write mechanism, the diodes do not use the wavelengths that would directly interact with either the P or Q intermediate. Therefore, the described write scheme has inherently negligible, if any, erasure; that is, it is nondestructive with respect to any previously written information. In contrast, erasure of an adjacent track by a stray field or the field generated by part of the recording head is one of the most critical issues in modern magnetic recording technologies.⁴⁸

Read Mechanism

The read process in the 2D case is substantially more straightforward and probably more economical than the popular read processes used in the 3D case. In the 2D case, no paging is necessary, because every bit of information can be read back with one shot (step) and the coordinates of the bit are determined by the location of the read element, as shown in Figure 8. This implies that, to precisely track the position of the bits, data servo methods similar to those employed in conventional magnetic and optical disk drives could be implemented.

The two most obvious ways to read information from the protein disk rely on

the difference between the two binary states in absorption maxima and amounts of fluorescence.

Reading through absorption measurements is possible because the two binary states, the bR and P/Q states, have quite different absorption maxima, as shown in Figure 5. Thus, the read signal could be chosen as either reflected or transmitted power, as shown in Figure 8a or 8b, respectively.⁴⁹ For example, if a red diode with a wavelength of 593 nm is used as the source, then the signal detected by the photodiode, which needs to operate at the same wavelength, will depend on whether the protein in the bit region is in the bR or P/Q state. Because the bR state absorbs substantially more signal, the detected reflected or transmitted signal will be smaller for the bR case (binary 0) than the P/Q state (binary 1).⁵⁰ To enhance the signal, the disk substrates can be made to be opaque and reflective for the cases of reflection and transmission, respectively. Ideally, one would expect twice as much signal difference (between the two states) in the case of reflection because the effective distance through which the light passes in the disk is twice as long as it would be in the case of transmission. However, for the same reason, the absolute

value of the signal might also be weaker and, therefore, more noise-sensitive in the case of reflection. Consequently, to maximize the signal-to-noise ratio (SNR), it is critical to consider this wavelength-sensitive tradeoff, which depends on the thickness of the medium and the optical density of the protein film under study.

It has been predicted theoretically that fluorescence-based reading could be more efficient, that is, provide a factor-of-two higher SNR, than equivalent absorption-based reading.⁵¹ In these calculations, the shot noise was considered as the main source of noise because of the finite number of photons involved in the read process.⁵² This assumption is indeed valid for measurements with conventional scanning near-field optical microscope (SNOM) systems, which must operate with inadequately low power values (on the order of a fraction of a nanowatt, when over 100 nW is required to achieve an SNR of above 15 dB). In this particular study, because of the implementation of the nanolaser technology described in the next section, the authors obtained substantially higher power values, and therefore, the relative contribution to the SNR of the shot noise could be greatly diminished. Nevertheless, the mechanism of reading through fluorescence is different and therefore should be experimentally explored with regard to this project before any definite conclusions can be drawn about the most efficient implementation of protein-based disk drives.

In the case of fluorescence measurements, the detection assembly should operate at a characteristic wavelength of the fluorescent light (and not necessarily at the wavelength of the near-field source). Fluorescence detection is usually performed in the range from ultraviolet to red light wavelengths, that is, from ~150 nm to 650 nm.⁵³ When excited by a near-field source at a certain wavelength, an intermediate of BR undergoes a certain excitation and relaxation sequence, which, in turn, triggers fluorescence with a certain wavelength spectrum. It appears that different intermediates have different fluorescence spectra and therefore could be distinguished from each other.⁵⁴ Consequently, the detection assembly could be chosen to function at an independent wavelength at which the difference in the amount of fluorescence between the two binary states of BR is at its maximum.

Key Challenge in the Design of Write and Read Transducers

The key challenge to accomplish any of the above-described write and read

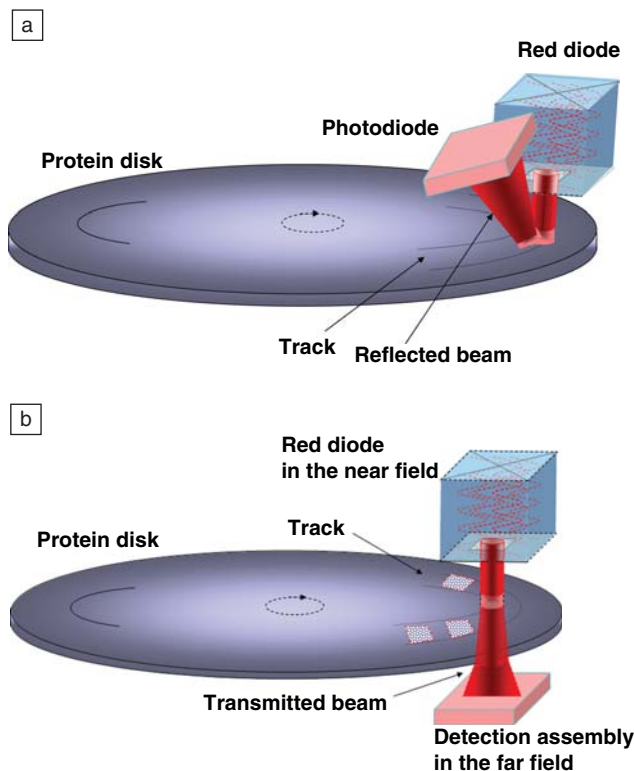


Figure 8. Schematics (not to scale) of protein disk recording systems with signal detection in the (a) reflection and (b) transmission modes.

mechanisms is to provide adequate (for a required SNR, i.e., 10–20 dB) power in a nanoscale beam spot.⁵⁵ Probably the most traditional way to image (read) information recorded in photochromic films would be similar to the mechanism used in scanning near-field optical microscopy (SNOM). By this, we mean not the relatively slow positioning through 2D or 3D piezoactuators used in conventional scanning probe microscopy (SPM) tools but rather the truly refined optical system used in SNOM. Indeed, the optics of state-of-the-art SNOM systems is capable of delivering record-low signal power (~0.1 nW) into a focusing spot size on the order of 30 nm. Literally, a few photons at different frequencies could be controlled in the near-field region. However, such relatively low power values are not adequate for implementing either of the recording processes, especially at room temperature, where thermal noise becomes a prevalent factor. In fact, to generate an adequate SNR (of ≥ 15 dB), it is estimated (through computer simulations) that the power of the light focused into a nanoscale spot with a diameter of ~30 nm should be on the order of hundreds of nanowatts, or at least 1,000 times higher than what could be produced by commercial SNOM systems.^{56,57}

The reason for the low power-delivery capability (throughput) of commercial SNOM systems is the use of fiber probes with modified tips. The ideal dimensions of the fiber are such that the light is propagated with no detectable power loss due to the existence of the waveguide conditions. However, to focus light into a nanoscale spot size (≤ 30 nm), the region close to the tip of the fiber should be modified accordingly. Now, if the light is delivered to a spot size substantially smaller than the wavelength, the waveguide in the region of the modified tip cannot comply with the waveguide conditions. As a result, over 99% of the energy (generated by the source) is lost on its way through the region of the modified tip. This explains the relatively inefficient energy-delivery capability (low throughput) of a fiber with a modified nanoprobe. Barely enough for reading, such a low power throughput is not at all adequate for writing information in protein films.

Solution to the Power Loss Problem in the Near-Field Optical Regime

To address the issue of inadequately low energy throughput of near-field systems, researchers worldwide have studied several near-field designs.^{58,59} Among the popular designs are tapered fibers with a

nonzero aperture, bow-tie antennas,⁶⁰ and so called “apertureless” probes (metal-coated diode lasers with a nanoscale aperture attached to an air-bearing surface of a recording head). Numerical simulations have indicated that the apertureless design might be the most efficient alternative.^{61,62} However, until recently, no experiment had been conducted to demonstrate power values above a few nanowatts (for a 30-nm aperture). The main challenge was associated with the complexity of fabricating and testing such small optical transducers.⁶³

Fortunately, the problem was recently resolved with the development of focused-ion-beam-(FIB)-fabricated high-throughput nanolasers at University of California–Riverside.⁶⁴ Based on the results of simulations with the commercial software ComSol to consider thermal effects in the near field as well,⁶⁵ Ikkawi et al. conducted a groundbreaking experiment to demonstrate the feasibility of nanolasers with output power in the near field finely controllable in the range from 0 to over 1 μ W.⁶⁶ The researchers used FIB to fabricate near-field optical transducers (nanolasers) with apertures as narrow as 10 nm.⁶⁷ A 100-nm-thick film of aluminum was coated on the emitting edge of a 5- μ W diode laser, and various aperture shapes were etched using FIB, as shown in Figure 9a. The emitting edge of the fabricated

nanolaser was scanned using SNOM. The power was collected by a platinum-coated silicon probe through a photon-multiplier tube (PMT) into an avalanche photodetector PIN-FET (*p*-intrinsic-*n* field-effect transistor). The light emitted by the nanolaser at every scan point was scattered by the vibrating silicon probe, and thus, the evanescent light in the near field was converted into propagating waves in the far field to then be detected by the PMT. The C-shaped aperture (with a 40-nm-long side) demonstrated the highest power, approximately 250 nW, focused into a spot size on the order of 30 nm (Figure 9b). The smallest power, approximately 160 nW, was demonstrated by the circular aperture. This technology is scalable to a beam diameter as narrow as 5 nm and powers ranging from 0 to above 1 μ W, and it is not sensitive to the wavelength of the diode. Therefore, it could be used for both the writing and reading mechanisms described previously.

A photograph of a commercial spindrive from Guzik Technical Enterprises⁶⁸ that was modified to conduct near-field and far-field optical experiments is shown in Figure 10. This photograph shows the system in transmission mode with the nanolaser in the near-field region and the detection assembly in the far field. The system can also be used in reflection mode with both fluorescence-

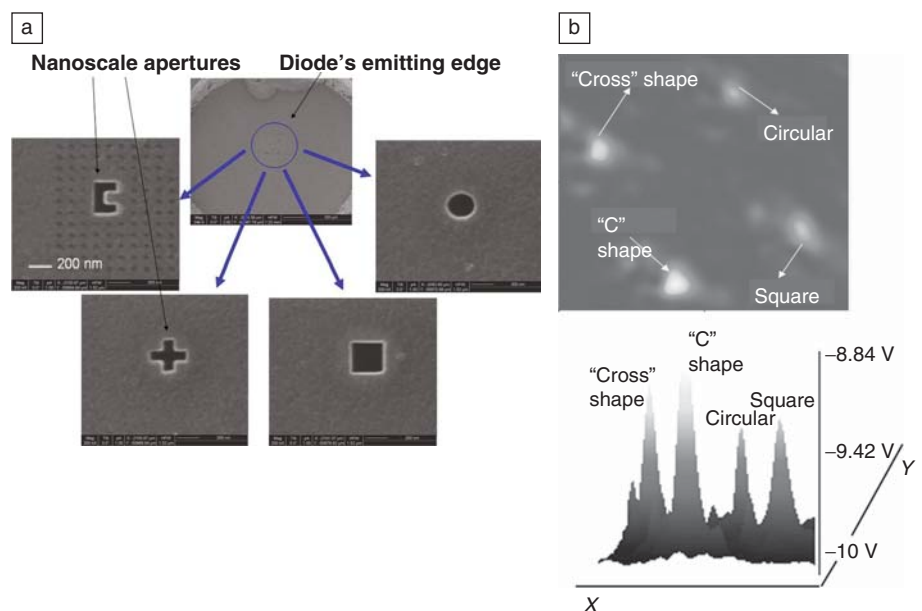


Figure 9. (a) Ion image of four different aperture shapes, namely, C-shaped, cross-shaped, circular, and square, etched by focused ion beam on the emitting edge of a diode laser. *Note:* The size marker is the same for all images in (a). (b) Scanning near-field optical microscope (SNOM) scan to demonstrate a nanolaser with a 40-nm C shape to focus light into a 30-nm spot. For comparison, SNOM images from the other three aperture shapes under study are also shown. To quantitatively compare the signals from the four aperture shapes, the digitized SNOM profiles for all four apertures are shown (bottom).

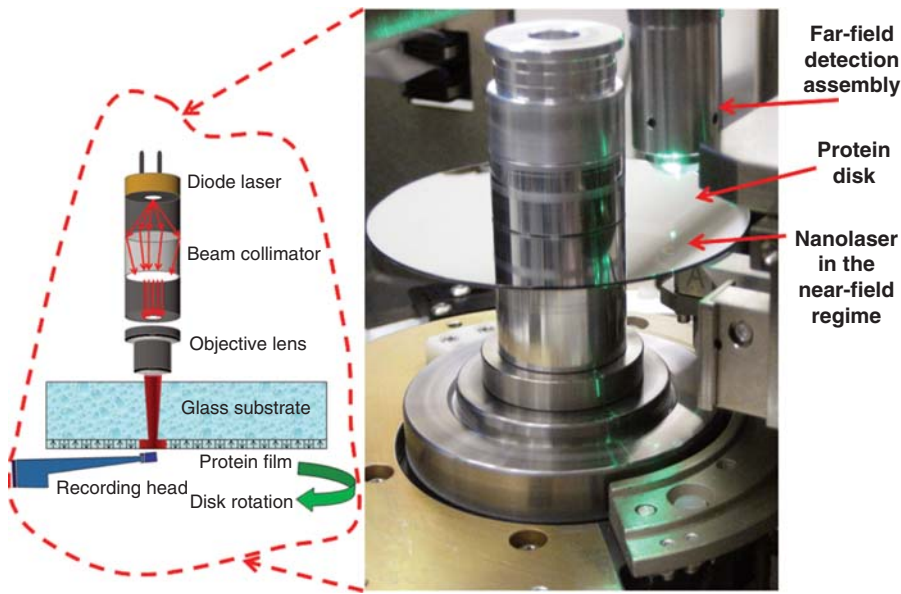


Figure 10. Photograph and schematic of a spindrive modified to conduct near-field and far-field optical experiments.

and absorption-based reading detection methods. The spindrive demonstration is the last step before the technology can be brought to the final commercialization stage.

Today, a number of laboratories throughout the world are able to coat disk substrates with protein films of various properties. However, it is often perceived that one of the main remaining challenges to be overcome before this technology can be commercialized is the development of thin overcoats. These overcoats are necessary to protect the protein films in the disk drive environment and to ensure an adequate lifetime of the memory device. Protein-based disk recording is one of the most promising technologies for the future of the multi-billion-dollar data storage industry. Companies have vast experience in solving technical issues associated with the development of thin overcoats and packaging into commercial devices. Eventually, this experience will be applied to the emerging technology of protein-based disk recording. In any recording disk implementation, overcoats act as both protective and lubrication layers. Therefore, the surface chemistry between potential overcoat materials and the protein should be thoroughly studied to maintain a separation of a few nanometers between the recording transducer and the protein film. In magnetic recording, the industry learned to keep the separation between the recording

head and the magnetic media (called "fly height") as small as 4 nm with an accuracy of less than 1 nm. There is every reason to believe that, with adequate chemistry, the same could be achieved also with protein disks.

Acknowledgments

The authors acknowledge research grants from the Office of Naval Research and the Defense Microelectronics Activity, particularly Award H94003-07-2-0703; the U.S. Air Force Office of Scientific Research; and the National Science Foundation. The authors also acknowledge the indispensable help of Andrey Lavrenov and Alexander Krichevsky with focused-ion-beam-based nanofabrication and near-field optical characterization, respectively. Finally, the authors acknowledge the invaluable support of William Cain from Western Digital Corporation.

References

1. S. Iwasaki, Y. Nakamura, *IEEE Trans. Magn.* **13**, 1272 (1977).
2. S. Khizroev, D. Litvinov, *Perpendicular Magnetic Recording* (Kluwer, Dordrecht, The Netherlands, 2005).
3. S.H. Charap, P.-L. Lu, Y. He, *IEEE Trans. Magn.* **33** (1), 978 (1997).
4. M. Albrecht, C.T. Rettner, A. Moser, M.E. Best, B.D. Terris, *Appl. Phys. Lett.* **81** (15), 2875 (2002).
5. C. Chappert, H. Bernas, J. Ferré, V. Kottler, J.-P. Jamet, Y. Chen, E. Cambril, T. Devolder,

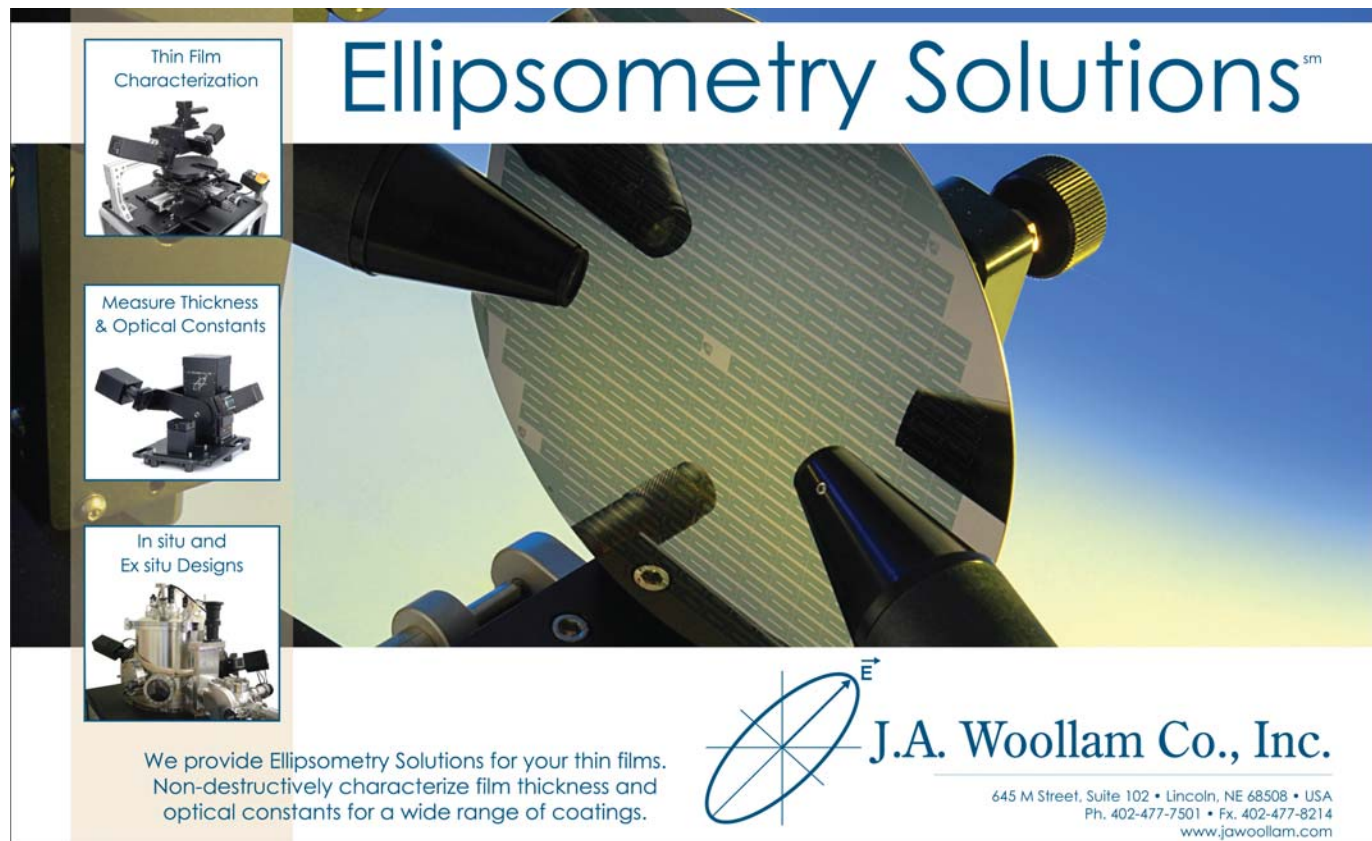
- F. Rousseaux, V. Mathet, H. Launois, *Science* **280**, 1919 (1998).
6. D. Weller, A. Moser, *IEEE Trans. Magn.* **35**, 4423 (1999).
7. H.F. Hamann, Y.C. Martin, H.K. Wickramasighe, *Appl. Phys. Lett.* **84** (5), 810 (2004).
8. P.C. Arnett, D.C. Cheng, S. Khizroev, D.A. Thompson, U.S. Patent No. 6,483,672 (IBM Almaden Research Center, November 19, 2002).
9. S. Khizroev, B.W. Crue, D. Litvinov, U.S. Patent No. 6,513,228 (Seagate Technology, February 4, 2003).
10. S. Khizroev, W. Crue, D. Litvinov, U.S. Patent No. 6,646,827 (Seagate Technology, November 11, 2003).
11. S. Khizroev, U.S. Patent Application 20060028766, filed February 9, 2006; 11/197,377, filed August 4, 2005, with provisional patent, 60/598,645, filed August 4, 2004.
12. S. Khizroev, Y. Hijazi, N. Amos, D. Doria, A. Lavrenov, R. Chomko, T.-M. Lu, D. Litvinov, *J. Nanoelectron. Optoelectron.* **1**, 1 (2006).
13. D.A. Thompson, J.S. Best, *IBM J. Res. Dev.* **44** (3), 311 (2000).
14. D. Oesterhelt, W. Stoeckenius, *Proc. Natl. Acad. Sci. U.S.A.* **70**, 2853 (1973).
15. R.E. Armstrong, J.B. Warner, "Biology and the Battlefield," in *Defense Horizons 25* (Center for Technology and National Security Policy, National Defense University, Washington, DC, March 2003).
16. S. Hunter, F. Kiamilev, S. Esener, D. Parthenopoulos, P.M. Rentzepis, *Appl. Opt.* **29**, 2058 (1990).
17. R.R. Birge, *Sci. Am.* **82**, 348 (1994).
18. R. Thoma, N. Hampp, *Opt. Lett.* **17** (16), 1158 (1992).
19. T. Tsujioka, F. Tazono, T. Harado, K. Kuroki, M. Irie, *Jpn. J. Appl. Phys.* **33**, 5788 (1994).
20. J.A. Stuart, D.L. Marcy, K.J. Wise, R.R. Birge, *Synth. Met.* **127**, 3 (2002).
21. R. Henderson, G.F.X. Schertler, *Philos. Trans. R. Soc. London, Ser. B* **326** (1236), 379 (1990).
22. A. Miniewicz, V. Renugopalakrishnan, in *Bionanotechnology: Proteins to Nanodevices*, V. Renugopalakrishnan, R.V. Lewis, Eds. (Springer, New York, 2006), chap. 12.
23. E.M. Landau, J.P. Rosenbusch, *Proc. Natl. Acad. Sci. U.S.A.* **93**, 14532 (1996).
24. J.L. Spudich, *Science* **288** (5470), 1358 (2000).
25. N. Hampp, A. Popp, D. Oesterhelt, C. Brauchle, European Patent EP 0 655 162 (1992).
26. V. Renugopalakrishnan, A. Strzelczyk, P.Z. Li, A.A. Mokhnatyuk, S.H. Gursahani, M. Nagaraju, M. Prabhakaran, H. Arjomandi, S. Lakka, *Int. J. Quantum Chem.* **95**, 625 (2003).
27. www.umass.edu/microbio/rasmol.
28. N. Grigorieff, T.A. Ceska, K.H. Downing, J.M. Baldwin, R. Henderson, *J. Mol. Biol.* **259**, 393 (1996).
29. E.G. Pebay-Peyroula, G. Rummel, J.P. Rosenbusch, E.M. Landau, *Science* **277**, 1676 (1997).
30. H. Luecke, H.T. Richter, J.K. Lanyi, *Science* **280**, 1934 (1998).
31. T. Oka, K. Inoue, M. Kataoka, Y. Yagi, *Biophys. J.* **88** (1), 436 (2005).
32. G. Varo, J.K. Lanyi, *Biochemistry* **30** (20), 5016 (1991).

33. T. Rink, M. Pfeiffer, D. Osterhelt, K. Gerwert, H.-J. Steinhoff, *Biophys. J.* **78**, 1519 (2000).
34. A. Campion, J. Terner, M.A. El-Sayed, *Nature* **256**, 659 (1977).
35. S.P. Balashov, *Isr. J. Chem.* **35**, 415 (1995).
36. A. Popp, M. Wolperdinger, N. Hampp, C. Brauchle, D. Oesterhelt, *Biophys. J.* **65**, 1449 (1993).
37. G. Varo, J.K. Lanyi, *Biochemistry* **30**, 5008 (1991).
38. M. Wolperdinger, N. Hampp, *Biophys. Chem.* **56**, 189 (1995).
39. Actilor GmbH, www.mib-biotech.de.
40. R.R. Birge, U.S. Patent 5,559,732 (1994).
41. C. Denis Mee, E.D. Daniel, *Magnetic Recording* (McGraw-Hill, New York, ed. 2, 1996).
42. J.C. Mallinson, *The Foundation of Magnetic Recording 2E* (Academic Press, New York, ed. 2, 1993).
43. R.S. Muller, T.I. Kamis, M. Chan, *Device Electronics for Integrated Circuits* (Wiley, New York, ed. 3, 2002).
44. R.R. Birge, *Sci. Am.* **82**, 349 (1994).
45. N. Hampp, *J. Chem. Rev.* **100** (5), 1755 (2000).
46. F. Pina, *J. Am. Chem. Soc.* **119**, 5556 (1997).
47. D.W. McCamant, P. Kukura, R.A. Mathies, *J. Phys. Chem. B* **109** (20), 10449 (2005).
48. E. Svedberg, D. Litvinov, R. Gustafson, S. Khizroev, *J. Appl. Phys.* **93** (3), 2828 (2003).
49. K. Bagley, G. Dollinger, L. Eisenstein, A.K. Singh, L. Zimanyi, *Proc. Natl. Acad. Sci. U.S.A.* **79** (16), 4972 (1982).
50. P.J. Booth, A. Farooq, *Eur. J. Biochem.* **246** (3), 674 (1997).
51. T. Tsujioka, M. Irie, *Appl. Opt.* **37** (20), 4419 (1998).
52. R. Sarpeshkar, T. Delbruck, C.A. Mead, *IEEE Circuits Devices Mag.* **23** (November 1993).
53. N.B. Gillespie, L. Ren, L. Ramos, H. Daniel, D. Dews, K.A. Utzat, J.A. Stuart, C.H. Buck, R. Birge, *J. Phys. Chem. B* **109** (33), 16142 (2005).
54. Y. Yokoyama, M. Sonoyama, S. Mitaku, *J. Biochem.* **131**, 785 (2002).
55. D. Sarid, presented at INSIC Annual Meeting, Monterey, CA, 2002.
56. T. Tsujioka, M. Irie, *Appl. Opt.* **38**, 5066 (1999).
57. A. Partovi, D. Peale, M. Wuttig, C.A. Murray, G. Zydzik, L. Hopkins, K. Baldwin, W.S. Hobson, J. Wynn, J. Lopata, L. Dhar, R. Chichester, J.H.-J. Yeh, *Appl. Phys. Lett.* **75**, 1515 (1999).
58. F. Chen, A. Itagi, J.A. Bain, D.D. Stancil, T.E. Schlesinger, *Appl. Phys. Lett.* **83** (16), 3245 (2003).
59. M.E. Itkis, F. Borondic, A. Yu, R.C. Haddon, *Science* (312), 413 (2006).
60. R.D. Grober, R.J. Schoelkopf, III, D.E. Prober, U.S. Patent 5,696,372 (December 9, 1997).
61. T. Milster, F. Akhavan, M. Bailey, J. Erwin, D. Felix, K. Hirota, S. Koester, K. Shimura, Y. Zhang, *Jpn. J. Appl. Phys.*, **1** (40), 1778 (2001).
62. X. Shi, R. Thornton, L. Hesselink, *Proc. SPIE* **4342**, 320 (2001).
63. F. Chen, A. Itagi, J.A. Bain, D.D. Stancil, T.E. Schlesinger, *Appl. Phys. Lett.* **83** (16), 3245 (2003).
64. P. Patel-Predd, *MITs Technol. Rev.* (November/December 2007).
65. www.comsol.com.
66. R. Ikkawi, N. Amos, A. Krichevsky, R. Chomko, D. Litvinov, S. Khizroev, *Appl. Phys. Lett.* **91** (15), 3115 (2007).
67. S. Khizroev, D. Litvinov, *Nanotechnology* **14**, R7-15 (2004).
68. www.guzik.com. □



MRS
materials360PLUS
www.mrs.org/360plus

**Materials News
 Materials Information
 Resources and Links
 Meetings Calendar
 and Much More!**



Ellipsometry SolutionsSM

Thin Film Characterization

Measure Thickness & Optical Constants

In situ and Ex situ Designs

We provide Ellipsometry Solutions for your thin films. Non-destructively characterize film thickness and optical constants for a wide range of coatings.

J.A. Woollam Co., Inc.

645 M Street, Suite 102 • Lincoln, NE 68508 • USA
 Ph. 402-477-7501 • Fx. 402-477-8214
www.jawoollam.com